Обзор ArXiv:astro-ph, 16-20 октября 2017 года

От Сильченко О.К.

Astro-ph: 1710.06441

THE EXTENT OF CHEMICALLY ENRICHED GAS AROUND STAR-FORMING DWARF GALAXIES

Sean D. Johnson,[1,2,*] Hsiao-Wen Chen,[3] John S. Mulchaey,[2] Joop Schaye,[4] and Lorrie A. Straka[4]

[1] *Department of Astrophysical Sciences, 4 Ivy Lane, Princeton University, Princeton NJ 08544, USA*
[2] *The Observatories of the Carnegie Institution for Science, 813 Santa Barbara Street, Pasadena, CA 91101, USA*
[3] *Department of Astronomy & Astrophysics, The University of Chicago, 5640 S. Ellis Ave., Chicago, IL 60637, USA*
[4] *Leiden Observatory, Leiden University, PO Box 9513, NL-2300 RA Leiden, the Netherlands*

Submitted to ApJL

ABSTRACT

Supernova driven winds are often invoked to remove chemically enriched gas from dwarf galaxies to match their low observed metallicities. In such shallow potential wells, outflows may produce massive amounts of enriched halo gas (circum-galactic medium or CGM) and pollute the intergalactic medium (IGM). Here, we present a survey of the CGM and IGM around 18 star-forming field dwarfs with stellar masses of $\log M_*/M_\odot \approx 8-9$ at $z \approx 0.2$. Eight of these have CGM probed by quasar absorption spectra at projected distances, d, less than the host virial radius, R_h. Ten are probed in the surrounding IGM at $d/R_\mathrm{h} = 1-3$. The absorption measurements include neutral hydrogen, the dominant silicon ions for diffuse cool gas ($T \sim 10^4$ K; Si II, Si III, and Si IV), moderately ionized carbon (C IV), and highly ionized oxygen (O VI). Metal absorption from the CGM of the dwarfs is less common and $\approx 4\times$ weaker compared to massive star-forming galaxies though O VI absorption is still common. None of the dwarfs probed at $d/R_\mathrm{h} = 1-3$ have definitive metal-line detections. Combining the available silicon ions, we estimate that the cool

Выборка: 18 маломассивных иррегулярных карликов…

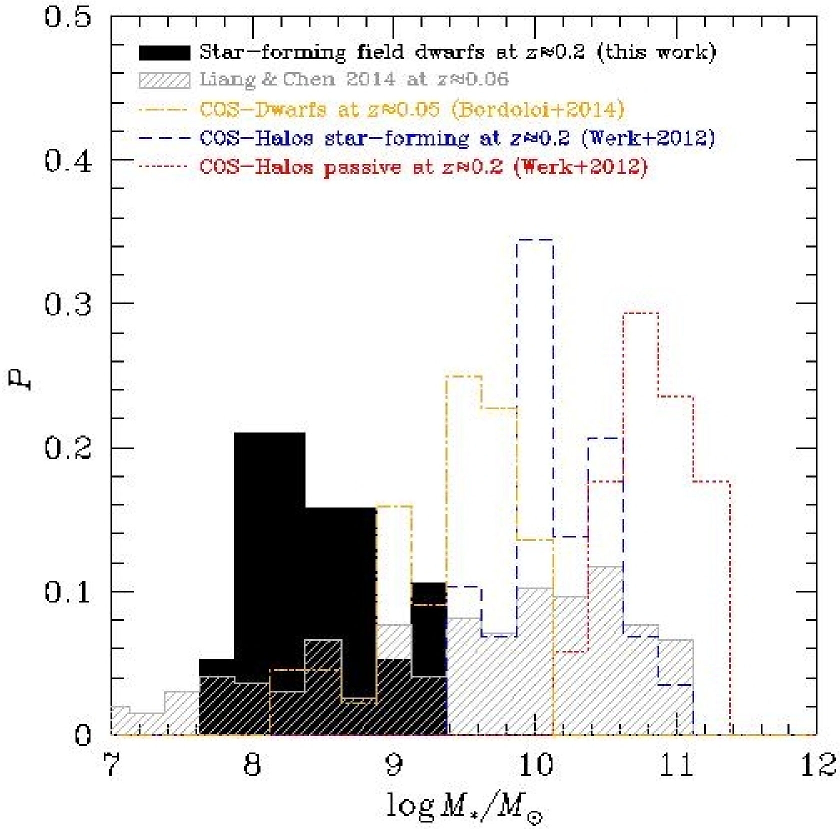

Figure 1. Stellar mass distribution of the star-forming field dwarf galaxies. For comparison, the star-forming and passive galaxies from the COS-Halos survey and intermediate mass samples from COS-Dwarfs and Liang & Chen (2014) are also shown.

… с квазарами на дальнем фоне

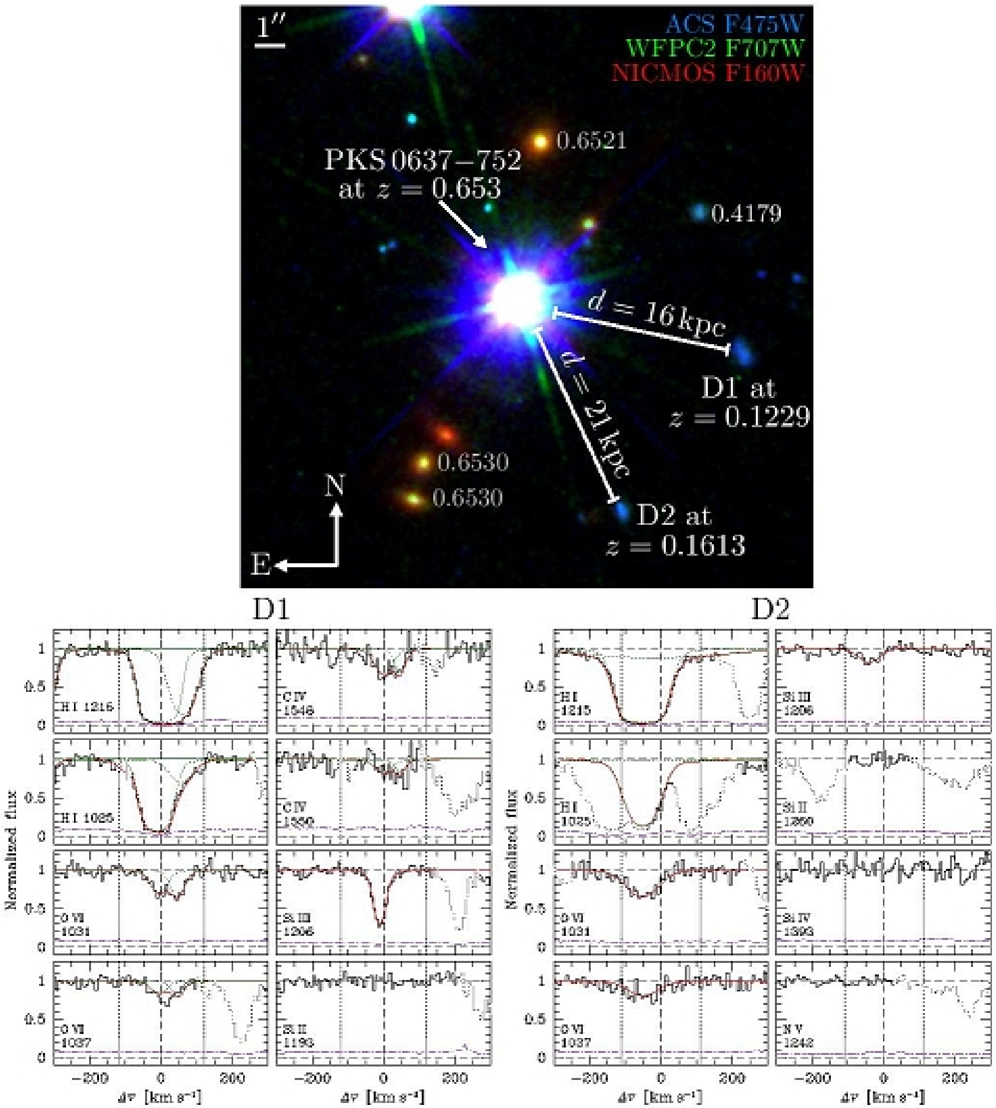

Figure 2. Examples of the star-forming field dwarf galaxies D1 and D2 near the sightline toward PKS 0637−752. The *top*

Результат

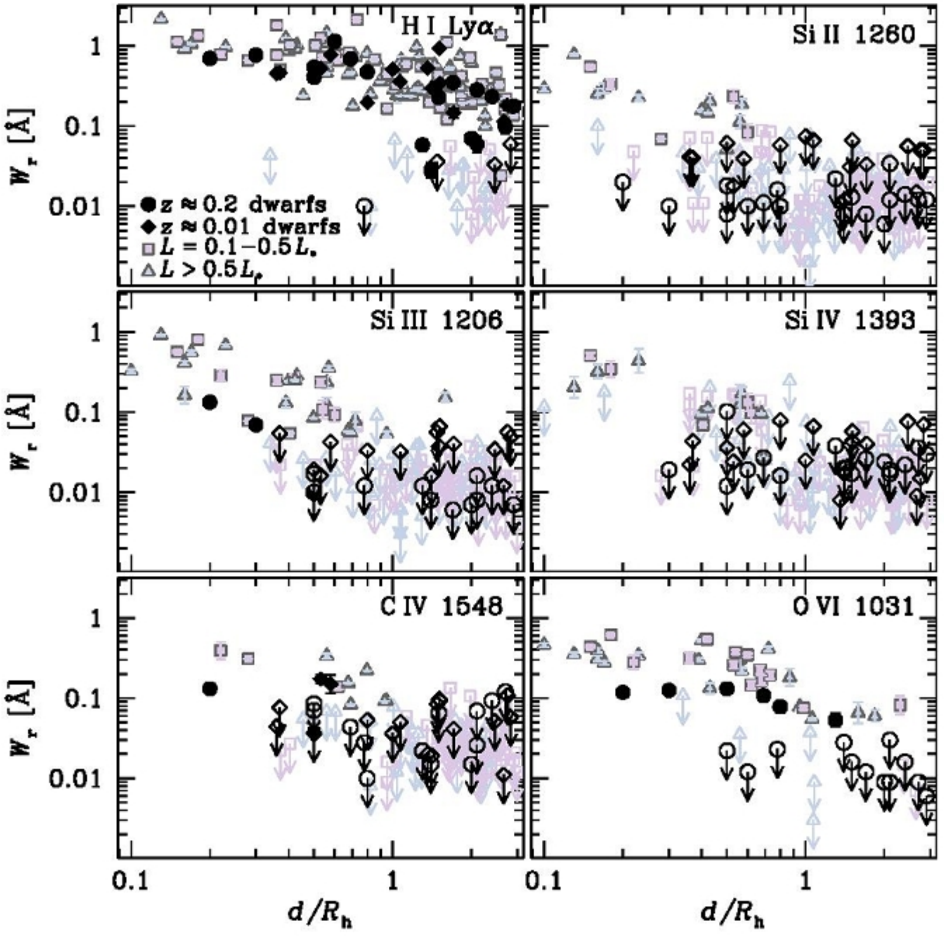

- Катастрофически не хватает металлов в окологалактическом пространстве;
- Их совсем нет на d/Rh>1;
- А на d/Rh=0.2-0.3 хорошо представлены только совсем высоковозбужденные ионы – OVI
- ГДЕ OUTFLOWS ОТ СВЕРХНОВЫХ??

Astro-ph: 1710.05034

SDSS IV MaNGA - sSFR profiles and the slow quenching of discs in green valley galaxies

Francesco Belfiore[1,2,3★], Roberto Maiolino[2,3], Kevin Bundy[1], Karen Masters[4], Matthew Bershady[5], Grecco Oyarzun[1], Lihwai Lin[6], Mariana Cano-Diaz[7], David Wake[8,9], Ashley Spindler[9], Daniel Thomas[4], Joel R. Brownstein[10].

[1] *University of California Observatories - Lick Observatory, University of California Santa Cruz, 1156 High St., Santa Cruz, CA 95064, USA.*
[2] *University of Cambridge, Cavendish Astrophysics, Cambridge, CB3 0HE, UK.*
[3] *University of Cambridge, Kavli Institute for Cosmology, Cambridge, CB3 0HE, UK.*
[4] *Institute of Cosmology and Gravitation, University of Portsmouth, Dennis Sciama Building, Portsmouth, PO1 3FX, UK.*
[5] *University of Wisconsin - Madison, Department of Astronomy, 475 N. Charter Street, Madison, WI 53706-1582, USA.*
[6] *Institute of Astronomy and Astrophysics, Academia Sinica, Taipei 106, Taiwan.*
[7] *Instituto de Astronomía, Universidad Nacional Autonóma de México, A.P. 70-264, 04510 México, D.F., Mexico.*
[8] *Department of Physics, University of North Carolina Asheville, One University Heights, Asheville, NC 28804, USA.*
[9] *The Open University, Walton Hall, Milton Keynes, MK7 6AA, UK.*
[10] *Department of Physics and Astronomy, University of Utah, 115 S. 1400 E., Salt Lake City, UT 84112, USA.*

Выборка

2.1 The MaNGA data

The MaNGA survey (Bundy et al. 2015; Yan et al. 2016b), part of SDSS-IV (Blanton et al. 2017), aims to obtain spatially resolved spectroscopy for a representative sample of 10 000 galaxies in the redshift range $0.01 < z < 0.15$ by 2020. The MaNGA instrument operates on the SDSS 2.5m telescope at Apache Point Observatory (Gunn et al. 2006) and consists of a set of 17 hexagonal fibre bundles of different sizes, plus a set of mini-bundles and sky fibres used for flux calibration and sky subtraction respectively (Drory et al. 2015; Law et al. 2015; Yan et al. 2016a). All fibres are fed into the dual beam BOSS spectrographs covering the wavelength range from 3600 Å to 10300 Å with a spectral resolution $R \sim 2000$ (Smee et al. 2013).

MaNGA galaxies are selected from an extended version of the NSA catalogue and are observed out to 1.5 R_e (primary sample, comprising 2/3 of the total sample) or 2.5 R_e (secondary sample, comprising 1/3 of the total sample). Targets are selected to be representative of the overall galaxy population at each stellar mass in the range $9.0 < \log(M_\star/M_\odot) < 11.0$ (in practice M_i is used for sample selection to avoid the systematic uncertainty intrinsic in deriving stellar masses, Wake et al. 2017).

The MaNGA data used in this work was reduced using version v1_5_1 of the MaNGA reduction pipeline (Law et al. 2016). Our starting sample consists of all MaNGA galaxies observed within the first ~ 2 years of operation, corresponding to the publicly available SDSS data release 13 (DR13, Albareti et al. 2016), which includes 1352 unique galaxies.

eLIER and line-less galaxies are defined to host no spectroscopically-detected star formation, and are thus excluded from the current study. We emphasize that in this work a galaxy is defined as SF based on its MaNGA spectroscopy and not by its position with respect to the SFMS, although, as seen in Fig. 2, galaxies classified as SF lies mostly on the SFMS.

For a reliable study of radial gradients we impose further cuts on our galaxy sample, as in Belfiore et al. (2017a). In detail we select galaxies to have a major to minor axis ratio (b/a) greater than 0.4 (to exclude high-inclination systems), $9.0 < \log(M_\star/M_\odot) < 11.5$ and exclude visually-classified mergers or closely interacting systems. These cuts lead to a final sample of 579 galaxies. The relative mix of blue cloud and GV, as well as SF and cLIER sources in this sample is detailed in Table 1.

Оценка специфического темпа звездообразования – по эмиссии H-alpha

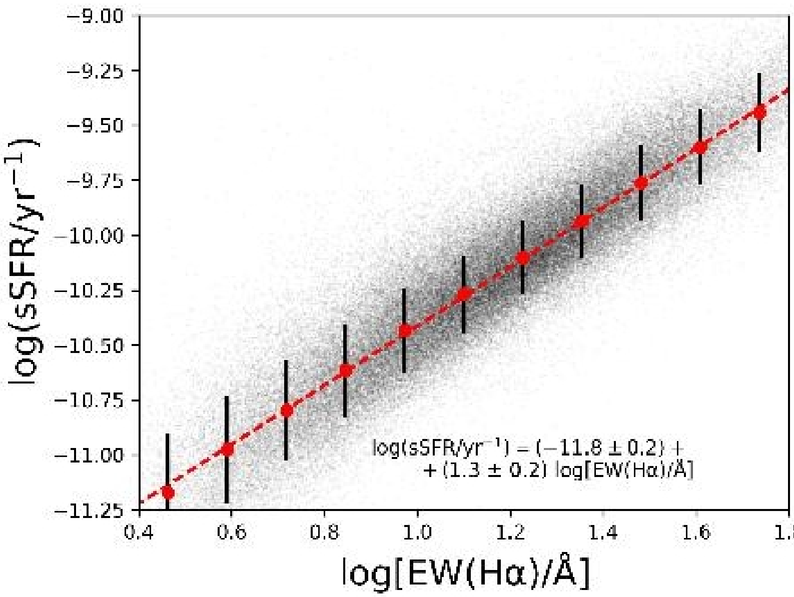

Figure 1. The relation between sSFR and EW(Hα) in emission for all the spaxels classified as star forming using the [SII]/Hα BPT diagram in the

Table 1. Sample of MaNGA galaxies used in this work.

Type	N. galaxies
Sample used in this work	579
Blue Cloud	443 (76%)
Green Valley (GV)	109 (19%)
Red Sequence	27 (5%)
star forming (SF)	455 (79%)
central LIER (cLIER)	124 (21%)

Veilleux & Osterbrock 1987; Kauffmann et al. 2003b; Kewley et al. 2006; Belfiore et al. 2016).

Using repeat observations Yan et al. (2016b) demonstrate that for log(SFR/$M_\odot$ yr^{-1} kpc^{-2}) > -2.7 (converting to a Chabrier IMF) and E(B − V) < 0.5 the uncertainty in the SFR is less than 0.2 dex. This uncertainty is dominated by the uncertainty in

Разделение голубого облака и зеленой долины

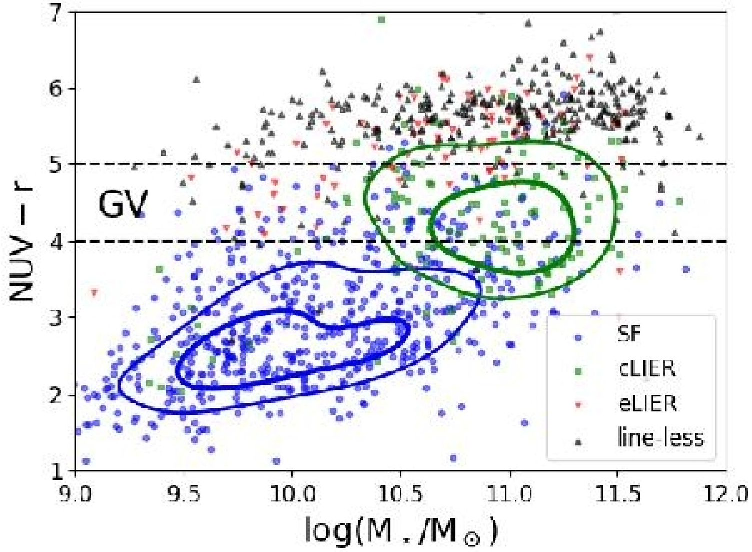

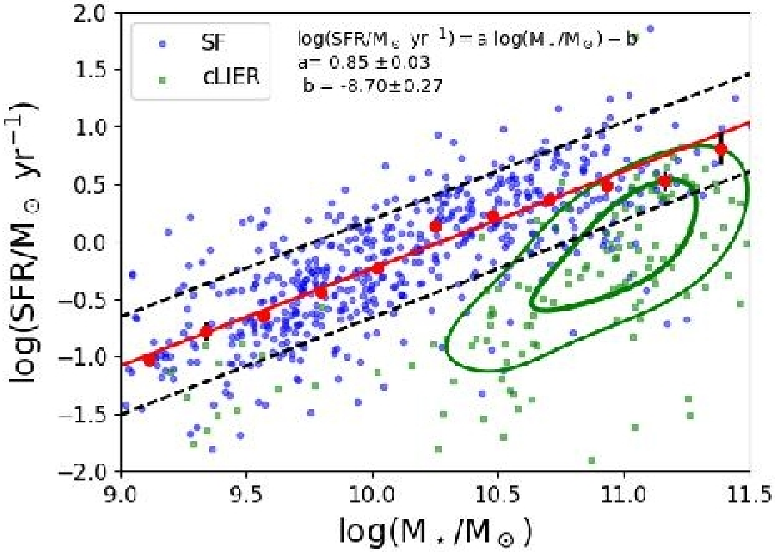

Результат

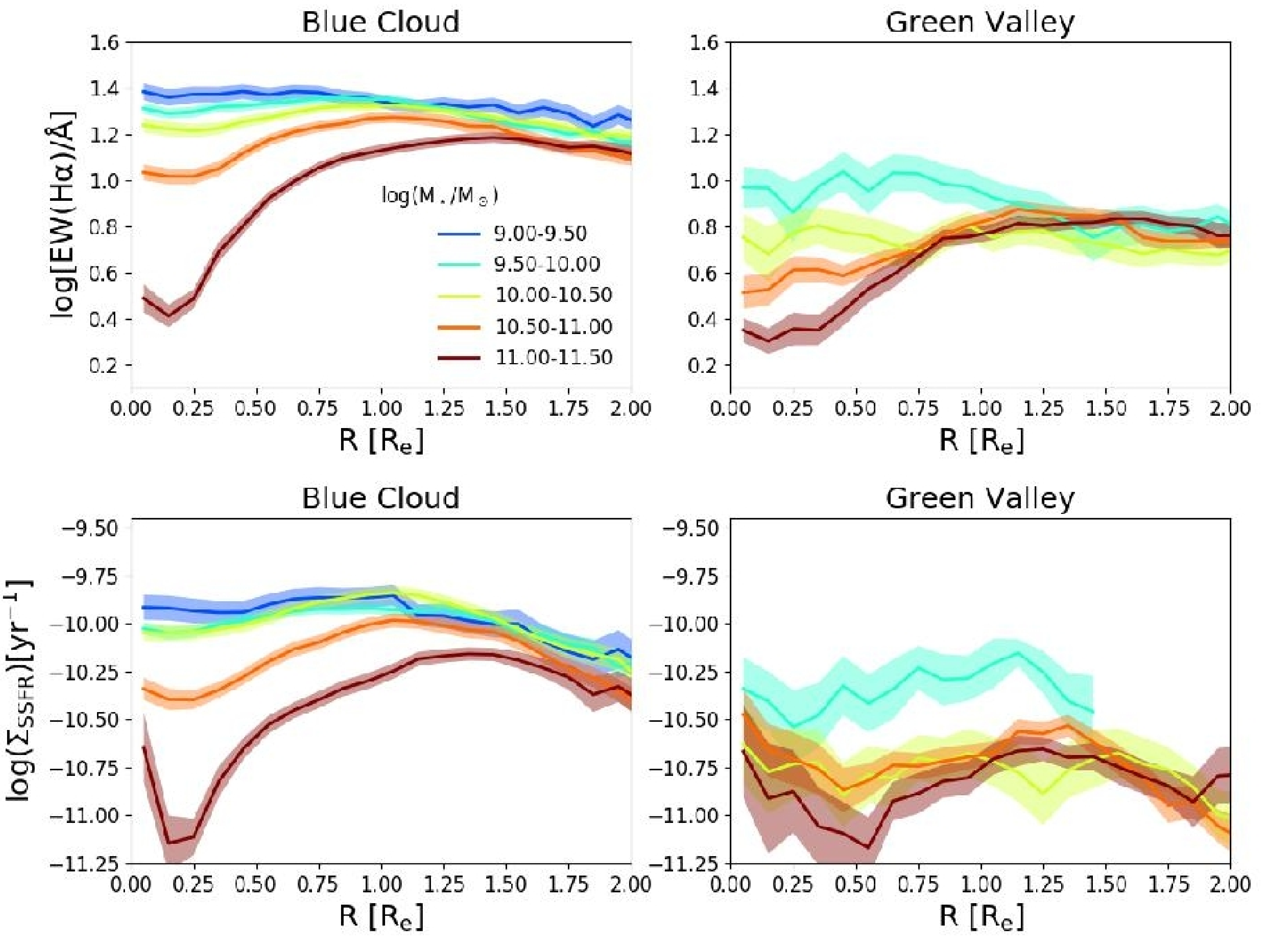

re 3. Top: The stacked EW(Hα) radial profiles for different mass bins in the blue cloud (left) and the GV (right). Profiles are computed by

В галактиках с «подавленным центром» звездообразование подавлено и по всему диску!

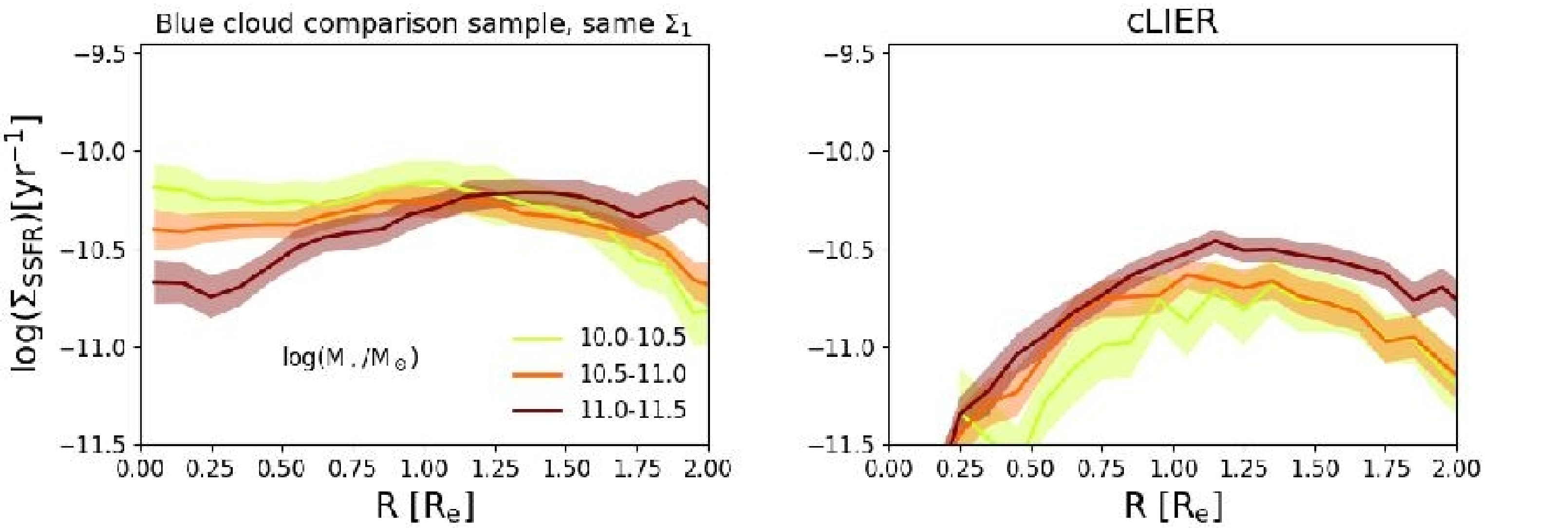

Figure 7. Same as Fig. 6, but comparing the cLIER sample with a sample of star forming galaxies matched in mass and Σ_1 (the stellar mass surface density within 1 kpc, as defined in Fang et al. 2013). The comparison demonstrates that GV galaxies have lower sSFR in their discs even when compared to a sample of blue cloud galaxies with comparable total mass and central mass surface density (Σ_1).

Astro-ph: 1710.05049

SDSS-IV MaNGA: The Spatial Distribution of Star Formation and its Dependence on Mass, Structure and Environment

Ashley Spindler[1★], David Wake[1,2], Francesco Belfiore[3], Matthew Bershady[4], Kevin Bundy[3], Niv Drory[5], David R. Law[6] Karen Masters[7], José R. Sánchez-Gallego[8], Daniel Thomas[7], Kyle Westfall[3], Vivienne Wild[9]

[1] *The Open University, Walton Hall, Milton Keynes, MK7 6AA, UK.*
[2] *Department of Physics, University of North Carolina Asheville, One University Heights, Asheville, NC 28804, USA.*
[3] *University of California Observatories - Lick Observatory, University of California Santa Cruz, 1156 High St., Santa Cruz, CA 95064, USA*
[4] *Department of Astronomy, University of Wisconsin, 475 N. Charter St., Madison, WI 53706, USA.*
[5] *McDonald Observatory, University of Texas at Austin, 1 University Station, Austin, TX 78712-0259, USA.*
[6] *Space Telescope Science Institute, 3700 San Martin Drive, Baltimore, MD 21218, USA* [7] *Institute of Cosmology and Gravitation, University*
[8] *Department of Astronomy, Box 351580, University of Washington, Seattle, WA 98195, USA.*
[9] *School of Physics and Astronomy, University of St Andrews, North Haugh, St Andrews, KY16 9SS, UK.*

Выборка: SDSS/DR14, 2791 галактика, из них

A final cut is applied to the sample based on galaxy axis ratio. Edge-on disks with a $b/a < 0.3$ are removed from the sample, as we have found that their radial profiles are poorly resolved. A total of 128 galaxies are removed based on this cut. The final sample is then composed of 1494 galaxies, 1016 of which are star forming, 364 are composite and 114 are AGN/LI(N)ER.

Особенности анализа:

- Классификация типа возбуждения – по ИНТЕГРАЛЬНОМУ спектру.
- По биннированому «Voronoi», S/N>20, калибровали оценку темпа звездообразования по скачку D4000.
- Результирующие картинки – по НЕбинированным изображениям.

Оценки темпов SF в индивидуальных спакселях

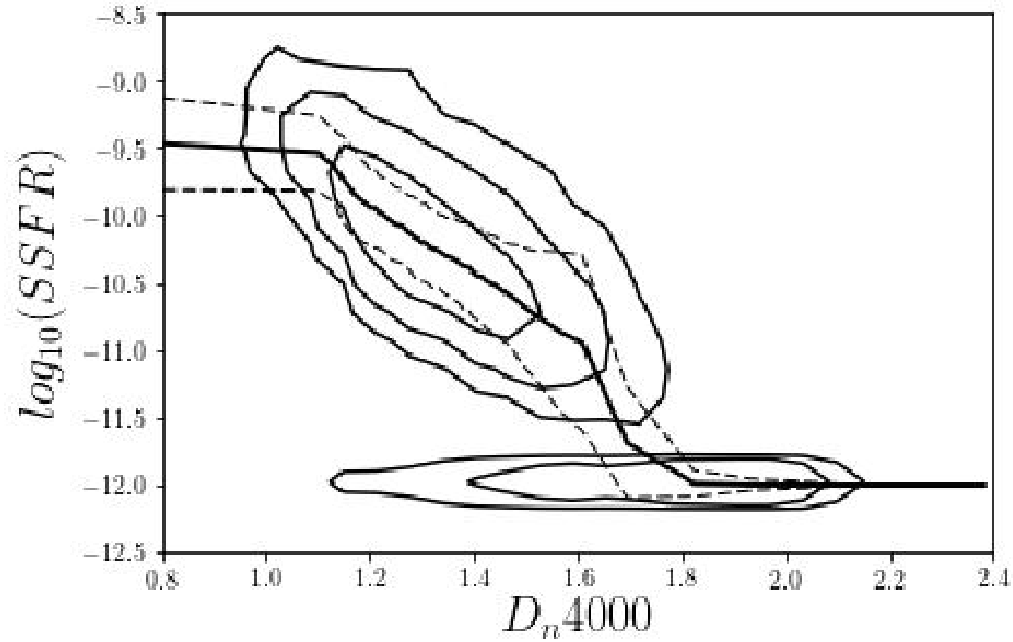

Figure 2. Contours of the distribution of D_n4000 and SSFR, the contours represent the 1−, 2− and $3-\sigma$ levels. The thick solid line is the mean fitted to the data we use for spaxels which are marked as composite or AGN/LINER from the BPT Diagram. Spaxels which we classify as low SNR are included in this model with an upper limit of $\log_{10}(SSFR) = -11.5$. The dashed lines are the standard deviation from the mean.

Радиальные профили SF в зависимости от массы:

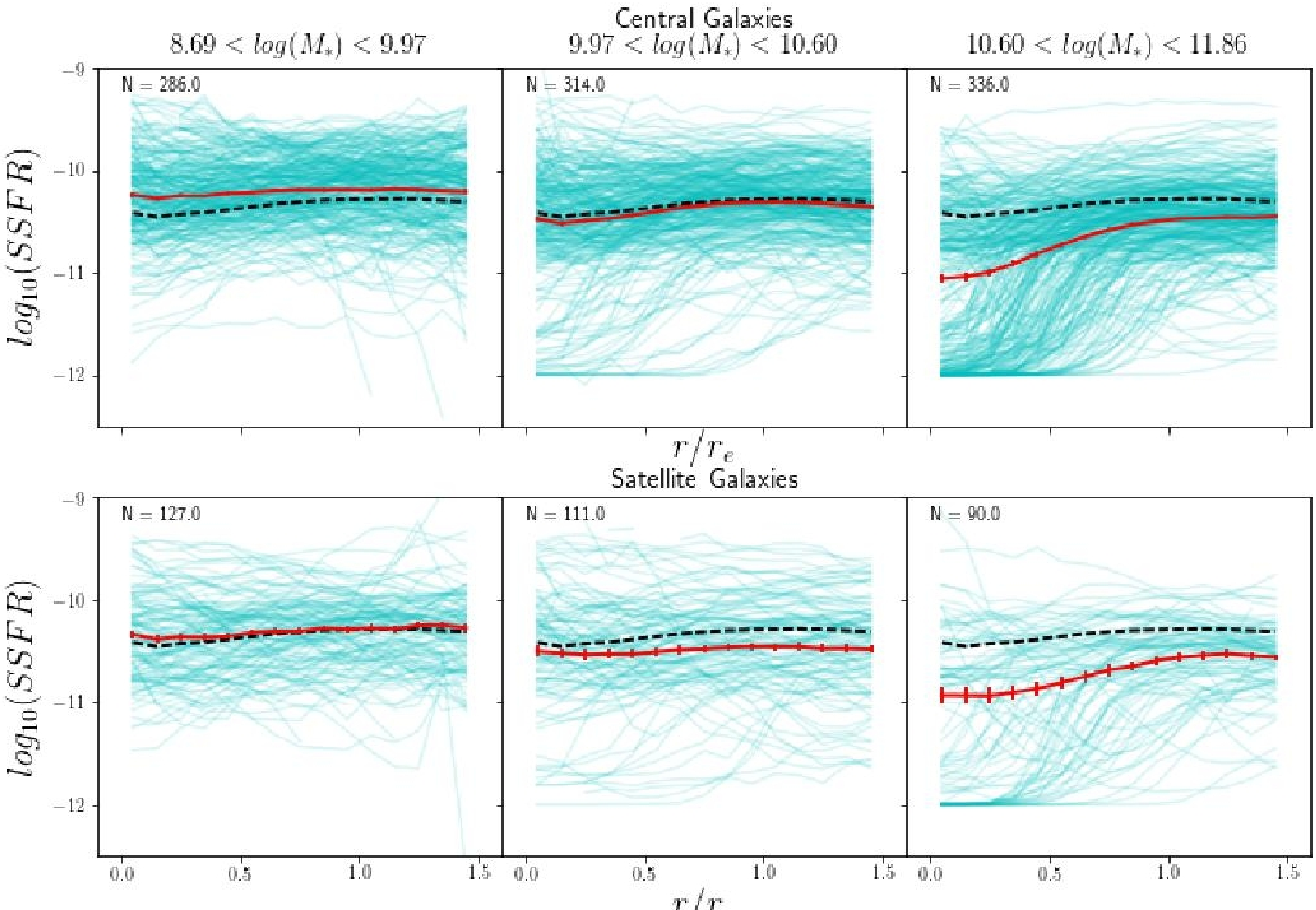

Сведено на одну картинку:

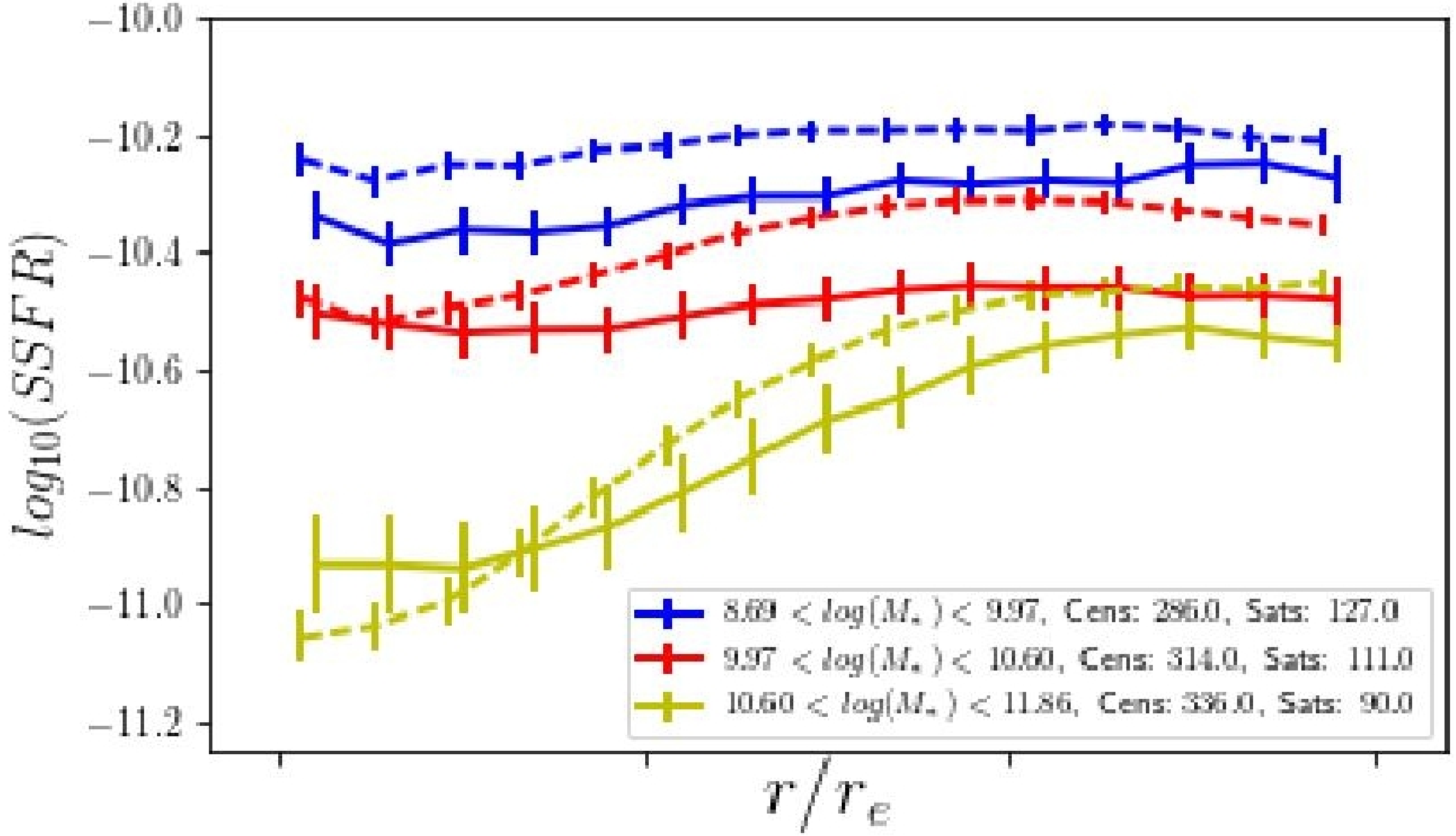

Радиальные профили SF в зависимости от центральной дисперсии скоростей:

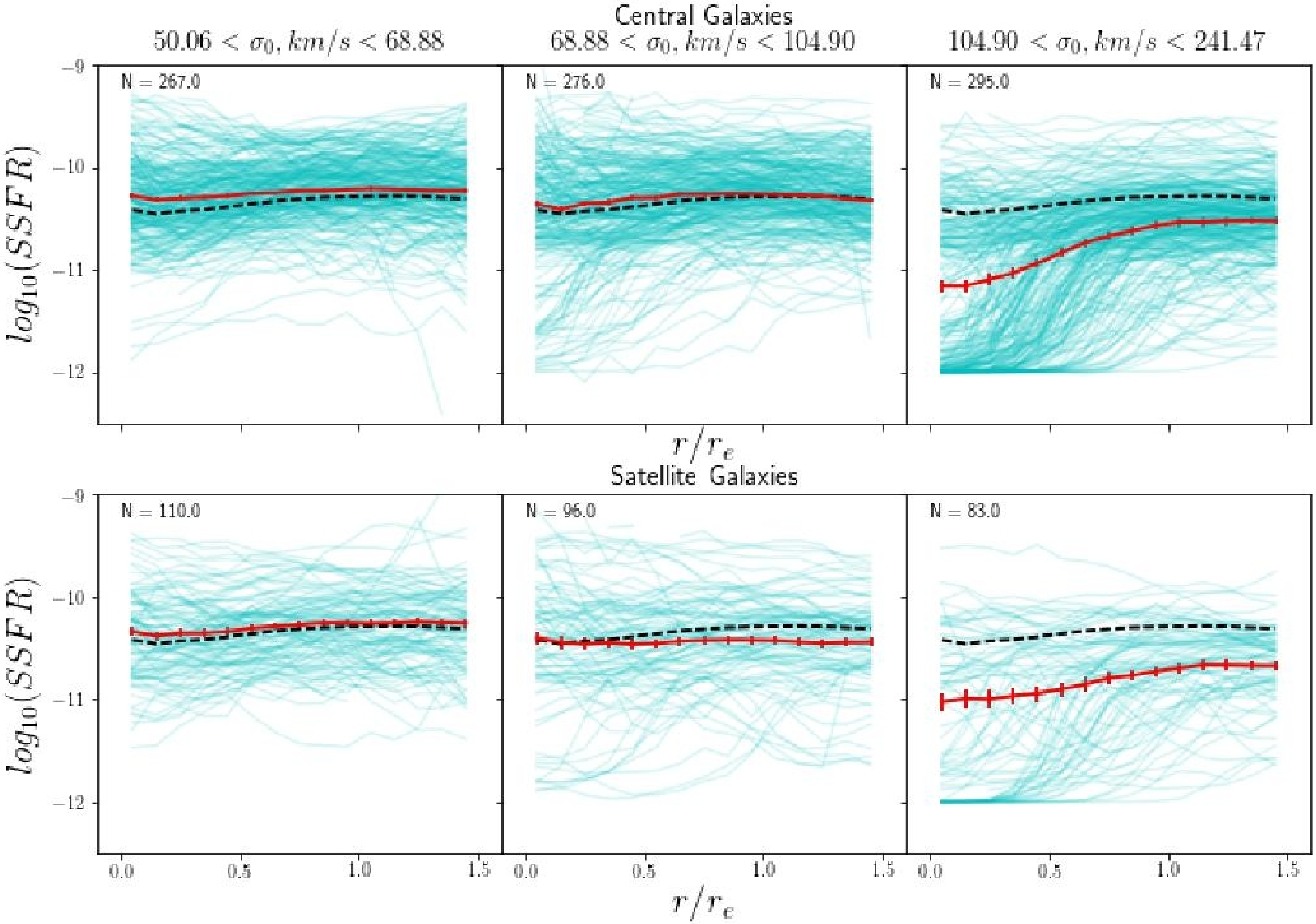

Сведено на одну картинку:

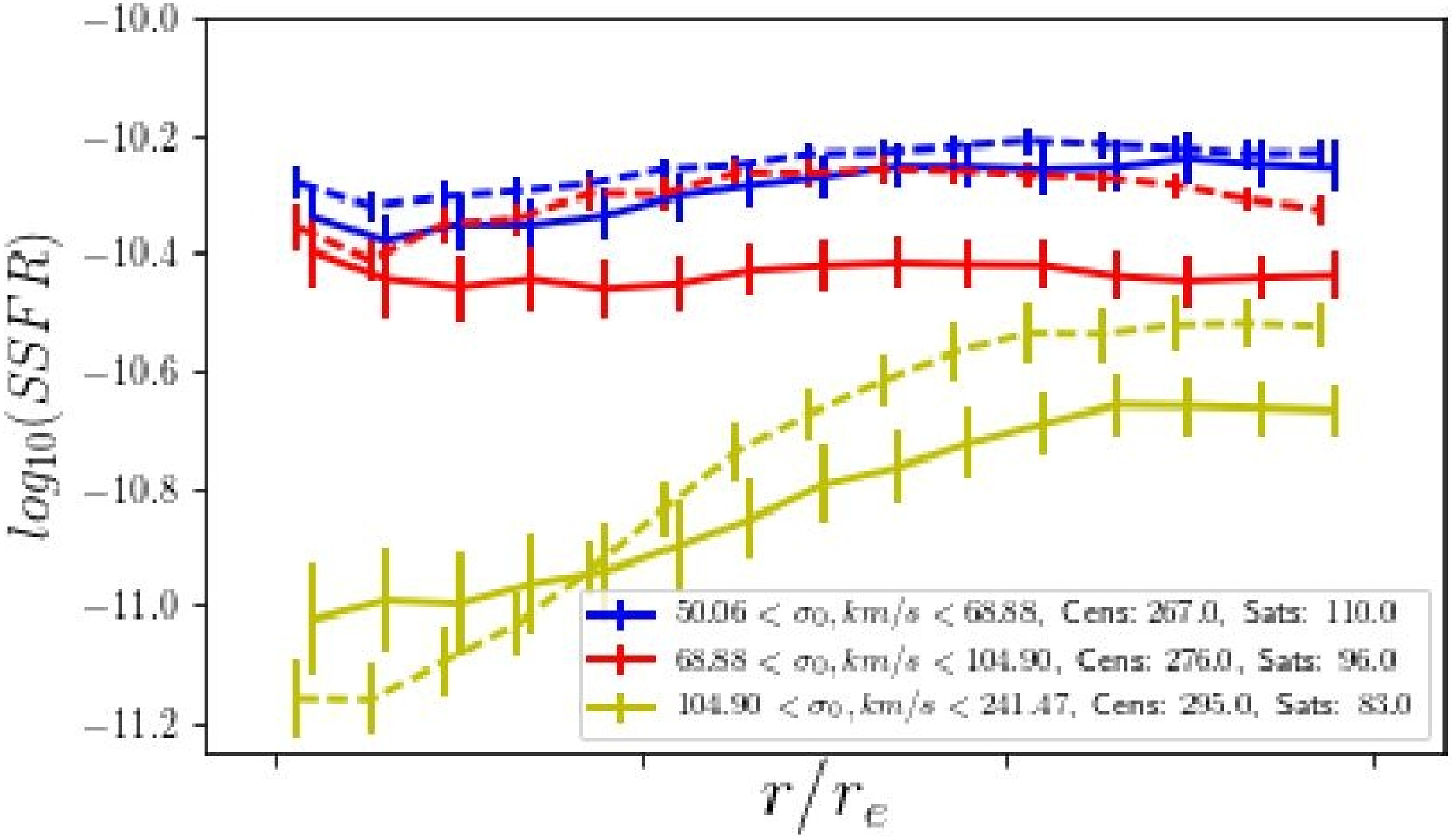

Разделение на имеющих «центральное подавление» и не имеющих:

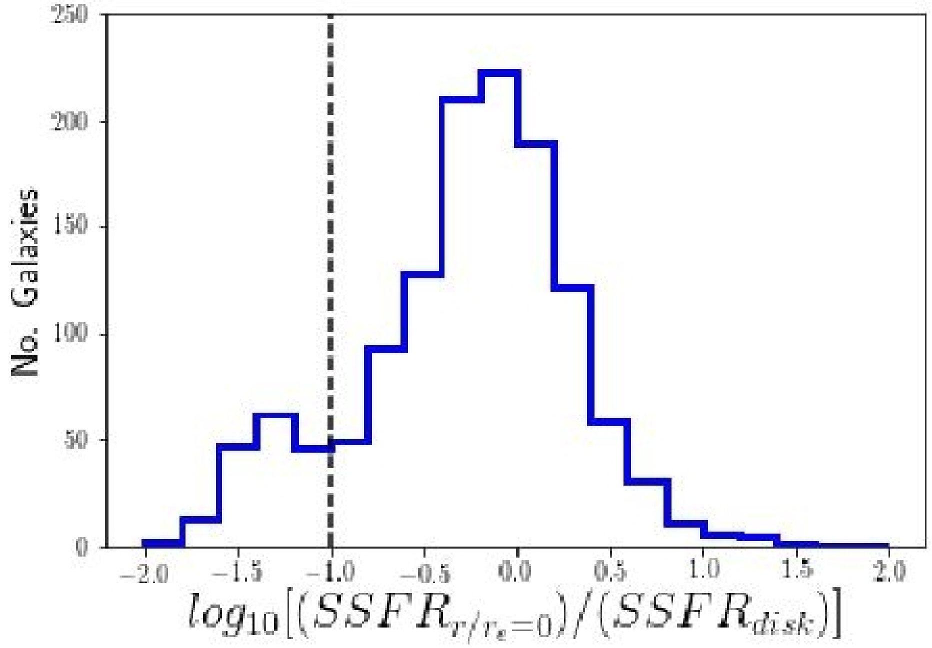

Figure 8. Histogram showing the ratios between the SSFR in the centre most radial bin and the mean SSFR beyond $r/r_e = 0.75$. We show with a dashed line the cut between the centrally suppressed and unsuppressed galaxies, which marks where the disk has SSFR is approximately 10 times higher than the core of the galaxy.

Центральное подавление играет бОльшую роль, чем масса и окружение?

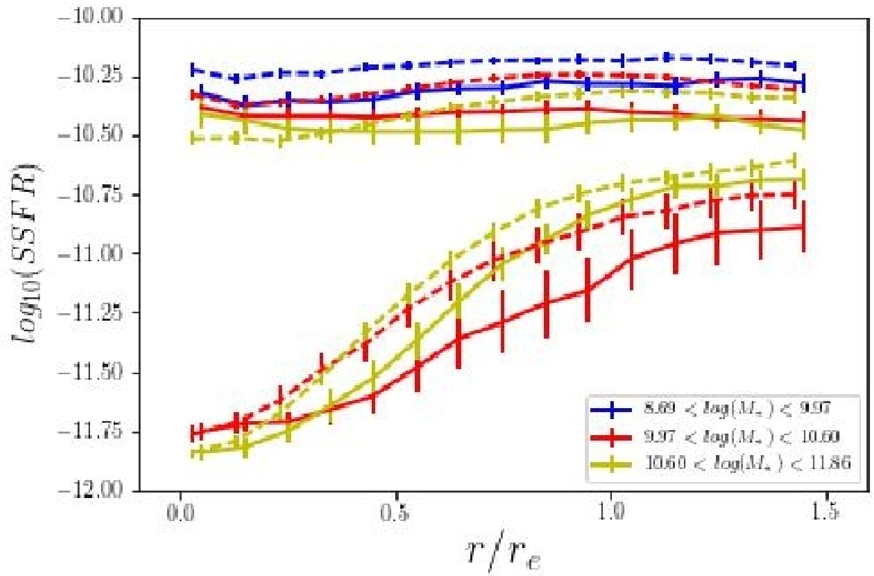

Figure 14. The mean SSFR profiles of centrally suppressed and unsuppressed galaxies. The upper set of lines are the unsuppressed galaxies, while the lower lines are the suppressed galaxies. Satellite profiles use solid lines and centrals use dashing lines. We do not include the low mass bin for the suppressed galaxies. We used the same three stellar mass bins as in Figure 6.

Доля «центрально-подавленных» не зависит от окружения!

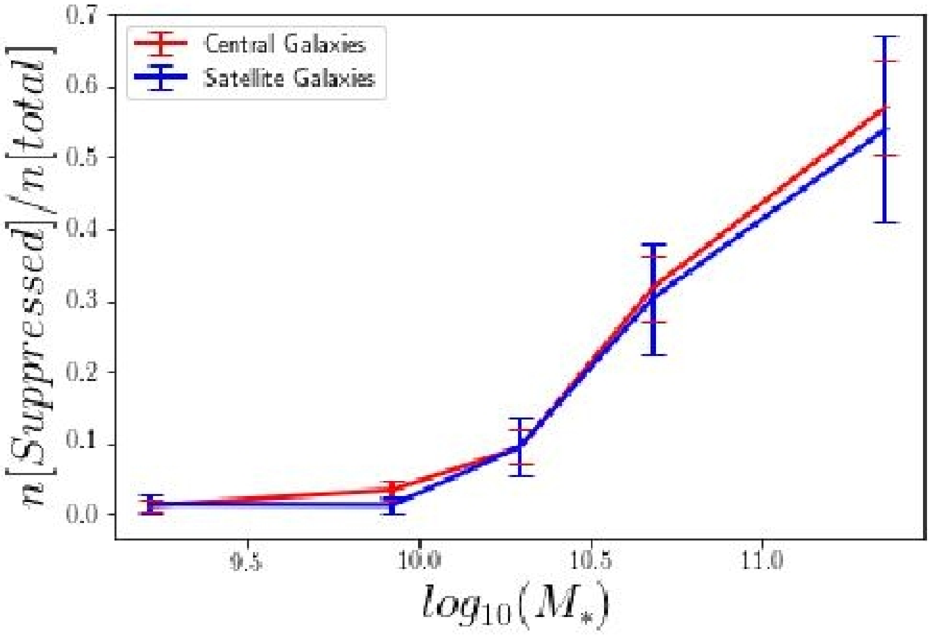

Figure 12. We show the fraction of centrals (red) and satellites (blue) which are centrally suppressed, with respect to Stellar Mass.

А от чего она зависит?

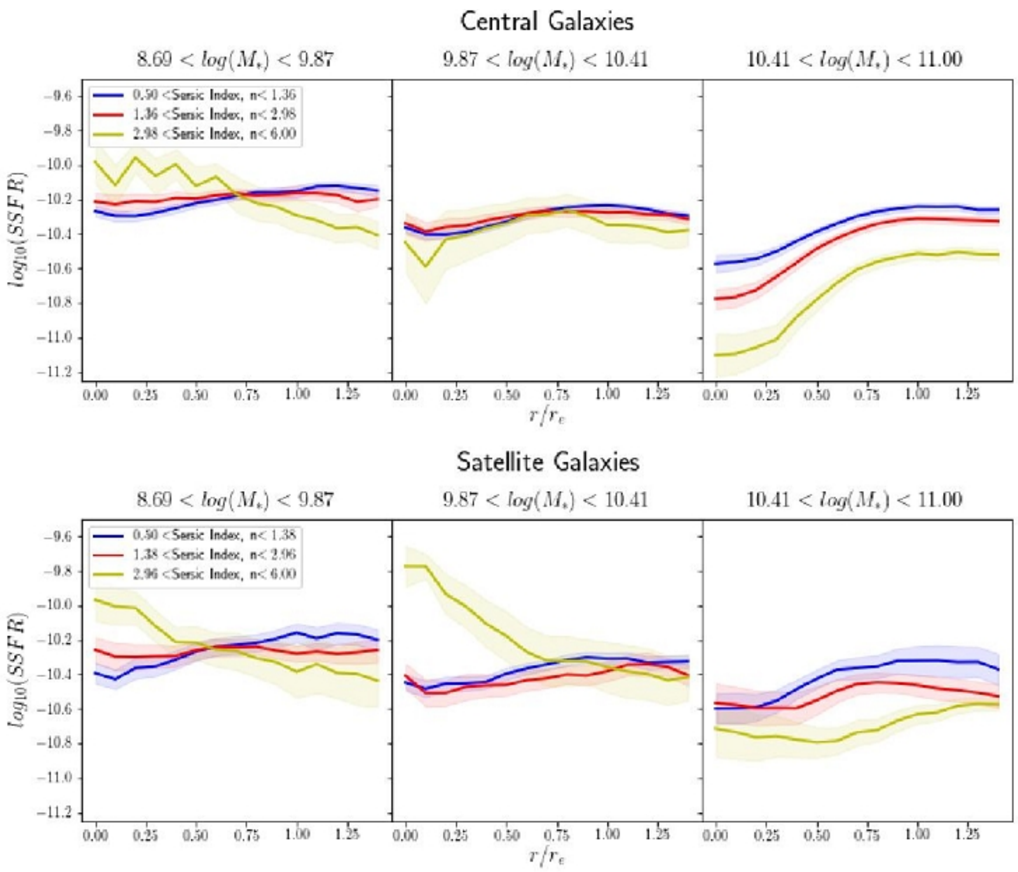

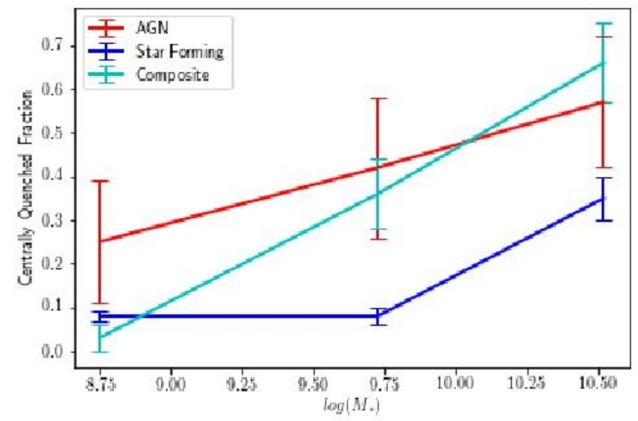

Figure 17. The fraction of galaxies which are centrally quenched, for galaxies which have an integrated BPT classification of AGN, Star Forming and Composite, in three bins of Stellar Mass.

Они считают, что это AGN